Charge-orbital ordering and ferroelectric polarization in multiferroic $TbMn_2O_5$ from first principles

Tay-Rong Chang,[1] Horng-Tay Jeng,[1,2,*] Chung-Yuan Ren,[3,†] and Chen-Shiung Hsue[1]
[1]*Department of Physics, National Tsing Hua University, Hsinchu 30013, Taiwan*
[2]*Institute of Physics, Academia Sinica, Taipei 11529, Taiwan*
[3]*Department of Physics, National Kaohsiung Normal University, Kaohsiung 80201, Taiwan*
(Received 17 November 2010; revised manuscript received 19 May 2011; published 15 July 2011)

The electronic structure and ferroelectric polarization of multiferroic $TbMn_2O_5$ are investigated using the generalized gradient approximation (GGA) and the GGA plus on-site Coulomb interaction (GGA+U) methods. We find an insulating charge-orbital ordered ground state driven by octahedral and pyramidal local structures. Associated with the observed charge ordering, the frustrated magnetic structure creates polarizations in the presence of magnetostriction effect. On-site U leads to strong cancellations between the ionic and electronic part of polarizations, giving rise to a residual value of 83 nC/cm^2 consistent with experimental data. By analyzing the contributions from individual species, we demonstrate that the main part of the polarizations results from the pyramidal Mn ions. Most importantly, we find clear evidence indicating that the d_{z^2} orbital ordering on the pyramidal Mn^{3+} sublattice play important roles in the polarization.

DOI: 10.1103/PhysRevB.84.024421 PACS number(s): 75.85.+t, 77.80.−e, 75.25.Dk, 71.15.Mb

I. INTRODUCTION

Charge ordering (CO) and orbital ordering (OO) are intriguing phenomena observed in recent years.[1–3] CO, which charge carriers localize at certain ionic sites, is typically accompanied with OO that electrons condense in certain orbitals, forming real-space ordering. They are closely related to spin and lattice degrees of freedom and play important roles in the electronic, magnetic, and transport properties of transition-metal oxides. Besides these well-known effects concerning CO and OO, recent works show increasing evidence that CO and OO significantly correlate to the origin of the electric polarization in the novel multiferroic materials as well.[4,5]

Multiferroics are the materials in which magnetism coexists with ferroelectricity. The magnetic and ferroelectric orders originate, respectively, from breaking the time-reversal symmetry by local spins and from breaking the spatial inversion symmetry by noncentral symmetric structures. Pierre Curie proposed at the end of the 19th century the magnetoelectric effect by which these two mechanisms could intimately interplay with each other. This effect is, however, usually too small to be useful for a practical application. Ever since the recent discovery of the gigantic magnetoelectric effect in $TbMnO_3$ by Kimura *et al.*,[6] multiferroics such as $RMnO_3$ and RMn_2O_5 (R = rare earth or Y) have attracted broad interest in the past few years because of the intricate mechanism behind as well as the high potential in future spintronics.[6–9] More excitingly, a new breakthrough toward colossal magnetoelectricity was proposed very recently.[10]

$TbMn_2O_5$ crystallizes in the orthorhombic space group $Pbam$ containing four $Mn^{4+}_{oct}O_6$ octahedra and four $Mn^{3+}_{pyr}O_5$ pyramids[11] as depicted in Fig. 1. Unfortunately, the spontaneous electric polarization cannot develop in this centrosymmetric structure. Recent measurements on neutron diffraction,[8] x-ray scattering,[12] and infrared phonon spectra[13] all indicate that the crystal symmetry of $TbMn_2O_5$ should be lower than $Pbam$ in the multiferroic state. The newly proposed $Pb2_1m$ group allows for a macroscopic electric polarization along the crystal b axis.[7,8,13,14] First-principles calculations[15,16]

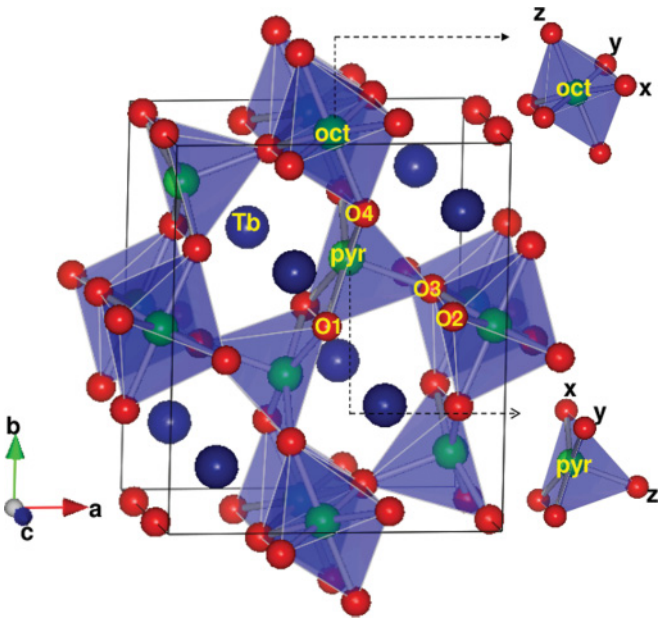

FIG. 1. (Color) Crystal structure of $TbMn_2O_5$. Blue, green, and red spheres denote Tb, Mn, and O(1–4) atoms, respectively. abc and xyz are, respectively, the crystal and local coordinates.

show a huge electric polarization of 1187 nC/cm^2,[15,16] which is orders of magnitude larger than the experimental value of ∼40 nC/cm^2.[7,8,14]

In this paper, we predict a charge-ordered insulating ground state associated with a d_{z^2} orbital ordering on the Mn^{3+}_{pyr} sublattices of $TbMn_2O_5$ from first-principles. The strong correlation effect is found to be crucial for obtaining correct electric polarization. We further resolve the close relation between the charge ordering and the polarization. In particular, we provide quantitative evidence to unravel the important roles that the orbital ordering plays in the polarization.

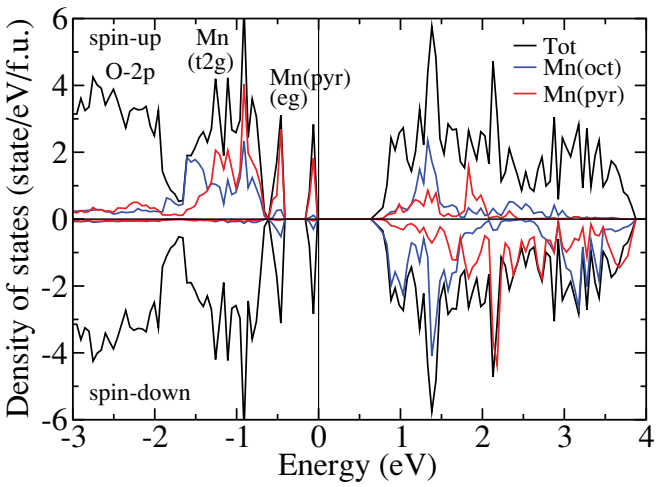

FIG. 2. (Color) Total DOS (black) of $TbMn_2O_5$ and site-decomposed DOS of Mn_{oct} (blue) and Mn_{pyr} (red) from the GGA. The Fermi level is at the zero energy.

II. COMPUTATIONAL DETAILS

The calculations are based on the generalized-gradient approximation (GGA)[17] and GGA plus Hubbard U (GGA+U)[18] using the full-potential projected augmented wave method[19] as implemented in the VASP package.[20] On-site $U = 1$–8 eV and exchange parameter $J = 0.8$ eV are used for all Mn ions. The $Pb2_1m$ structure (8 f.u., 64 atoms)[8,11] is optimized using a $2 \times 4 \times 6$ Monkhorst-Pack k-point mesh with a cutoff energy of 500 eV for different U separately. The optimized atomic forces are less than 1 meV/Å. The electronic polarizations are then calculated using the Berry-phase approach.[21,22]

III. Electronic Structure and Charge-Orbital Ordering

Figure 2 shows the GGA total and site-decomposed density of states (DOS). Similar to a previous work,[15] the GGA gives an insulating ground state with an energy gap of ~0.6 eV. The Mn $3d$ states dominate the energy band from E_F to ~ -1.7 eV, while the O $2p$ states are of lower energy. There exist two localized bands at -0.1 and -0.5 eV with a bandwidth of ~0.2 eV. Both bands originate mainly from Mn_{pyr} ions (Fig. 2), indicating the formation of the CO ground state in which Mn_{pyr} and Mn_{oct} are of, respectively, lower (nominally +3) and higher (nominally +4) ionicities. This CO state agrees qualitatively with the observed valences from neutron diffraction data.[11] Table I shows the integrated valence charge of Mn ions over the atomic spheres of radius 0.8 Å. The obtained charge disproportion between the electron-poor Mn_{oct} and the electron-rich Mn_{pyr} ions is about $0.1e$. Similar to the charge separations observed in other systems,[2] this value is far short of the nominal ionicity difference of $1e$ because of the strong screening effect. This CO state plays an important role in the ferroelectric polarizations, as will be discussed later. On the other hand, the spin ordering with moment separations of ~0.6 μ_B (Table I) between Mn^{4+}_{oct} ($t^3_{2g}\uparrow$) and Mn^{3+}_{pyr} ($t^3_{2g}\uparrow, e^1_g\uparrow$) (Ref. 23) agrees well with the observed moment difference from neutron diffraction experiment.[8]

TABLE I. Energy gap (eV), valence charge (e), and magnetic moment (μ_B) of the Mn ions within the atomic spheres of radius 0.8 Å in $TbMn_2O_5$.

	Gap	Charge Mn_{pyr}	Charge Mn_{oct}	Spin Mn_{pyr}	Spin Mn_{oct}
Expt.	1.7[a]	3.83[b]	2.98[b]	2.40[c]	1.81[c]
$U = 0$	0.6	3.72	3.64	2.82	2.22
$U = 6$	1.6	3.70	3.59	3.17	2.54

[a]Reference 24.
[b]Reference 11.
[c]Reference 8.

To clarify the origin of CO in $TbMn_2O_5$, we project the DOS onto the five $3d$ orbitals of Mn_{oct} and Mn_{pyr} ions in the local coordinates (xyz) indicated in Fig. 1. As shown in Figs. 3(a) and 3(b), both of the extra flat bands of Mn_{pyr} right below E_F are of d_{z^2} character with integrated charge of $0.58e$, whereas such bands are trivial in Mn_{oct}. This clearly indicates the formation of d_{z^2} OO in which the d_{z^2} orbital of Mn_{pyr} ion is approximately occupied by one electron while this orbital of Mn_{oct} ion is empty. Figure 3(c) shows the equal charge-density contour within the energy interval ($E_F \sim -0.6$ eV). The CO

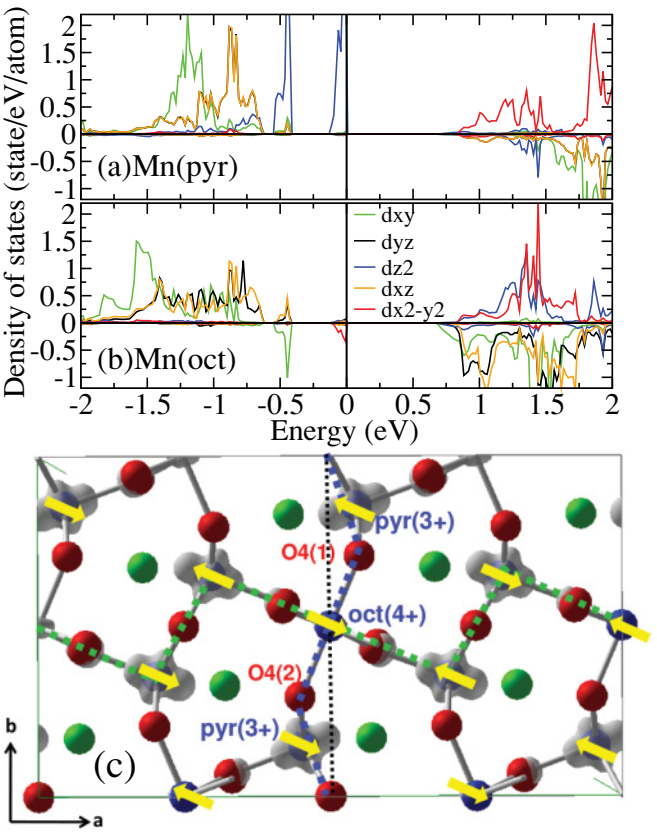

FIG. 3. (Color) DOS of $TbMn_2O_5$ projected onto the $3d$ orbitals of Mn_{pyr} (a) and Mn_{oct} ions (b). The Fermi level is at the zero energy. (c) Top view of the charge-orbital ordering pattern (gray) in the AFM $Pb2_1m$ unit cell of $TbMn_2O_5$. The blue, red, and green spheres denote Mn, O, and Tb, respectively. Yellow arrows denote the spin alignment. Green and blue dotted lines indicate the Mn-O chains along the crystal a and b directions, respectively.

and the associated d_{z^2} OO pattern is clearly seen: there exists exclusively an occupied d_{z^2} electron cloud on each Mn_{pyr} site. The Mn_{pyr} d_{z^2} OO actually plays an important role in electronic polarizations, as will be unveiled later.

Charge and orbital orderings have been found in many transition-metal oxides such as $La_{0.5}Sr_{1.5}MnO_4$,[1] Fe_3O_4,[2] and $SrRuO_3$.[3] In some cases, the on-site Coulomb energy U and/or Jahn-Teller (JT) distortions are crucial in the ordering formation. However, the main driving force in $TbMn_2O_5$ is the ligand fields rather than the on-site U or the Jahn-Teller distortions. Because of the octahedral crystal field in MnO_6 clusters, both of the e_g orbitals are of higher energy and are unoccupied. However, only one lobe of the d_{z^2} electron cloud endures the pyramidal ligand field from the apical O ion in the MnO_5 cluster. Consequently, the $Mn_{pyr}d_{z^2}$ orbital is energetically favorable, forming the charge-orbital ordering pattern in Fig. 3(c).

To examine if the local structure is the main driving force in the charge-orbital ordering formation in $TbMn_2O_5$, we performed several calculations such as GGA+U with or without JT distortion, ferromagnetic state, replacement of Tb by Ho and Dy, and even with spin-orbit coupling included self-consistently. They all lead to the same charge-orbital ordering pattern [Fig. 3(c)], indicating that the structural effect dominates all the other effects in the ordering formation.

Recent optical response measurement reveals strong anisotropy in dielectric functions.[24] They conclude that the main contributions to the strong anisotropy are the p-d charge transfer to the $d_{x^2-y^2}$ state in the $Mn^{3+}O_5$ pyramid, whereas it is of weak anisotropy from the octahedral $Mn^{4+}O_6$.[24] From our calculations, both the $d_{x^2-y^2}$ and d_{z^2} orbitals of Mn_{oct} are empty while only the $d_{x^2-y^2}$ state in Mn_{pyr} is unoccupied. Therefore, the spectral anisotropy from Mn_{pyr} is much stronger than that from Mn_{oct} in the OO state. This is in good agreement with the above experimental observations.

It is well known that the GGA largely underestimates the energy gap at E_F, especially for transition-metal oxides. The band-gap problem can be corrected by taking the on-site Coulomb repulsion U into account, as shown in Fig. 4(a). As U increases, the energy gap first grows more or less parabolically and then saturates with $U > 4$ eV. The gap size of $\sim$1.6 eV with $U = 4$–6 eV is in good agreement with $\sim$1.7 eV from near-band-gap absorption spectra,[24] indicating the importance of strong correlation effect. With $U > 6$ eV, the energy gap then deviates from the experimental value again. As a result, a reasonable on-site U would be from 4 to 6 eV.

IV. FERROELECTRIC POLARIZATIONx

The $Pbam$ lattice (Fig. 1) with inversion symmetry is actually polarization-prohibited. Neutron diffraction experiment[8] indicates a lower symmetry group $Pb2_1m$ with a doubled lattice constant a originated from the larger magnetic structure. As shown in Fig. 3(c), the antiferromagnetic (AFM) superexchange over Mn ion chains along the a direction (green-dotted line)[8,16] still reserves the inversion symmetry. In contrast, the frustrated "up-up-down" magnetic arrangement on $Mn^{\uparrow}_{pyr}$-$Mn^{\uparrow}_{oct}$-$Mn^{\downarrow}_{pyr}$ chains along the b direction (blue-dotted line) breaks the inversion symmetry.[16] With the magnetostriction effect that two magnetic ions of the same spin

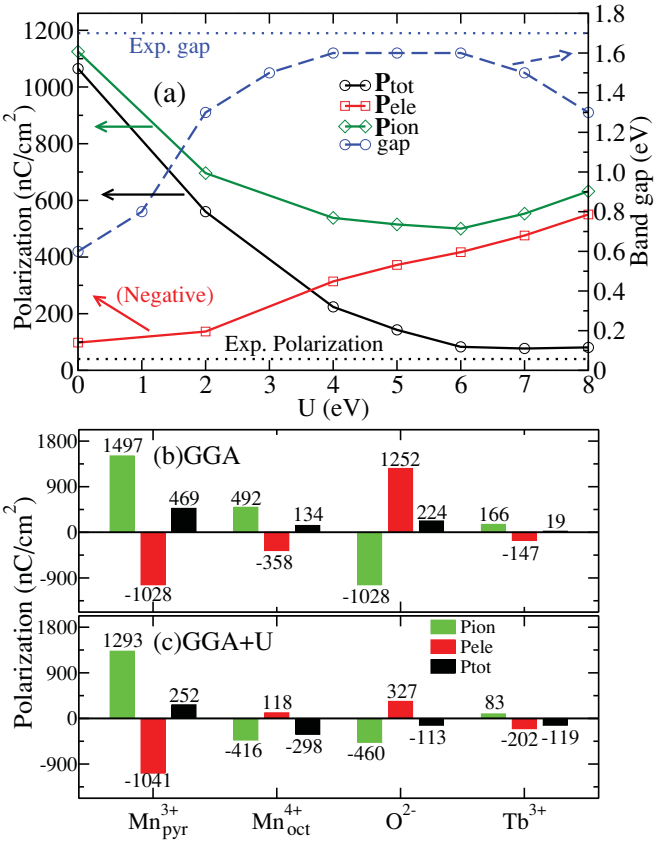

FIG. 4. (Color) (a) Energy gap (blue) at E_F, $\mathbf{P}_{tot}$ (black), $\mathbf{P}_{ion}$ (green), and negative $\mathbf{P}_{ele}$ (red) as a function of U. The lines are only a guide to the eye. The horizontal dotted lines denote the experimental values. "Site-decomposed" polarizations P_{tot} (black), P_{ion} (green), and P_{ele} (red) of different ions from GGA (b) and from GGA+U with $U = 6$ eV (c).

orientations tend to get closer whereas antiparallel spins prefer a farther separation for minimizing the exchange energy,[25] the unbalanced local dipoles in the CO state therefore give rise to an electric polarization.[4] Under GGA geometry optimization, the atomic distances $Mn^{\uparrow}_{pyr}$-$Mn^{\uparrow}_{oct}$ of 3.389 Å and $Mn^{\uparrow}_{oct}$-$Mn^{\downarrow}_{pyr}$ of 3.398 Å are, respectively, 0.011 and 0.020 Å longer than the undistorted[26] atomic distance of 3.378 Å. In fact, the GGA atomic distortion picture in which both Mn-Mn distances along b increase is inconsistent with the magnetostriction effect. This incorrect behavior will be further resolved later. The twice stronger displacement between Mn^{3+}_{pyr} and Mn^{4+}_{oct} in the later case hence gives rise to a total polarization ($\mathbf{P}_{tot}$) of 1027 nC/cm^2 along b. This is similar to 1187 nC/cm^2 from previous GGA calculations.[15,16] Nevertheless, both values are over 25 times larger than the experimental polarization of $\sim$40 nC/cm^2.[7,8,14]

The enormous discrepancy between the calculated and measured $\mathbf{P}_{tot}$ comes from the strong unbalance between the ionic ($\mathbf{P}_{ion}$) and electronic ($\mathbf{P}_{ele}$) part of polarization. The GGA ($U = 0$) $\mathbf{P}_{ion}$ of 1125 nC/cm^2 is one order of magnitude larger than $\mathbf{P}_{ele}$ of -98 nC/cm^2 [Fig. 4(a)]. The huge $\mathbf{P}_{ion}$ given by significant ionic displacements results from the overestimated intersite exchange forces. To estimate the magnetostriction strength, we calculate the atomic force by changing $Mn^{\downarrow}_{pyr}$

in the $Mn^{\uparrow}_{pyr}$-$Mn^{\uparrow}_{oct}$-$Mn^{\downarrow}_{pyr}$ chain along the b axis [Fig. 3(c)] to $Mn^{\uparrow}_{pyr}$. The spin flipping suddenly raises the zero atomic force on this Mn ion up to ~0.33 eV/Å. The sharply raised exchange force is presumably related to the over-binding problem in GGA calculations, whereas the small $\mathbf{P}_{ele}$ comes from a cancellation of polarizations from the Mn and O ions, as will be discussed later.

Figure 4(a) shows $\mathbf{P}_{tot}$, $\mathbf{P}_{ion}$, and negative $\mathbf{P}_{ele}$ as a function of U. The magnitude of $\mathbf{P}_{ele}$ grows monotonically with increasing U, while $\mathbf{P}_{ion}$ is significantly suppressed by U and attains its minimum at $U = 6$ eV. As a result, $\mathbf{P}_{tot}$ is drastically suppressed to 83 nC/cm^2 at $U = 6$ eV due to the strong cancellation between $\mathbf{P}_{ion}$ and $\mathbf{P}_{ele}$. In comparison with the huge value from the GGA, this is in excellent agreement with experimental data of ~40 nC/cm^2, indicating the importance of strong correlation in the electric polarization. A similar trend can also be found in $HoMn_2O_5$.[27] Since $\mathbf{P}_{ion}$ grows as $U > 6$ eV, $\mathbf{P}_{tot}$ thus saturates at ~80 nC/cm^2. Combined with the band-gap consideration, the best U would be ~6 eV.

The inclusion of U in the calculations leads to a relatively localized ionic picture and enhanced on-site exchange coupling (Table I) but suppressed intersite exchange interaction. Under geometry optimization with $U = 6$ eV, the bond lengths $Mn^{\uparrow}_{pyr}$-$Mn^{\uparrow}_{oct}$ of 3.370 Å and $Mn^{\uparrow}_{oct}$-$Mn^{\downarrow}_{pyr}$ of 3.387 Å are, respectively, 0.008 Å shorter and 0.009 Å longer than the undistorted[26] bond length of 3.378 Å. Using the above-mentioned spin-flip method, the obtained atomic force of ~0.16 eV/Å is only half of the GGA value. As a result, the smaller lattice distortions with correct magnetostriction behavior are the reason why $\mathbf{P}_{ion}$ is significantly inhibited by U.

The GGA actually gives a counterintuitive Mn-Mn distance picture in which both Mn-Mn distances increase. This unexpected behavior is related to the overbinding problem in the GGA scheme (relative to the GGA+U scheme) in which the intersite Coulomb and exchange interactions are stronger than they should be. Therefore, the lattice distortions are stronger than those in the GGA+U cases as discussed in the previous paragraphs. In our calculations, the GGA Mn-Mn bond distance distortions of 0.011 and 0.020 Å are larger than 0.008 and 0.009 Å from GGA+U. On the other hand, the bond-angle of Mn-O-Mn from GGA calculations,

$$\theta_{\uparrow\uparrow} = Mn^{3+}_{\uparrow}\text{-O-}Mn^{4+}_{\uparrow} = 123.36^{\circ},$$
$$\theta_{\downarrow\uparrow} = Mn^{3+}_{\downarrow}\text{-O-}Mn^{4+}_{\uparrow} = 124.49^{\circ},$$

are larger than those from GGA+U calculations with U of 6 eV,

$$\theta_{\uparrow\uparrow} = Mn^{3+}_{\uparrow}\text{-O-}Mn^{4+}_{\uparrow} = 120.73^{\circ},$$
$$\theta_{\downarrow\uparrow} = Mn^{3+}_{\downarrow}\text{-O-}Mn^{4+}_{\uparrow} = 121.44^{\circ}.$$

In comparison with the Mn-O-Mn bond angles in the undistorted FM states of 123.13° and 121.06° from GGA and GGA+U, respectively, one may find a similar trend to that of the bond length: The distorted bond angles are 0.23° and 1.36° larger than that of the undistorted one from the GGA, with one being 0.33° smaller and the other 0.38° larger than the GGA+U. Since the GGA+U intersite interactions are smaller, the lattice distortions are mainly along the crystal b direction, while distortions along a are negligible. Consequently, one may focus on the Mn-O-Mn chain along b only, and the correct Mn-Mn distance picture can be easily understood intuitively. However, in the GGA calculations with stronger intersite interactions, the lattice deforms not only along b but also along the a direction.[28] This makes the atomic distortions very complicated in the a-b plane. And this is also the reason why the GGA gives a counterintuitive Mn-Mn distance picture since the common intuition, which rises from one-dimensional considerations, is no longer suitable. Judging from the huge GGA polarization, which is far from close to the experimental observation, the GGA indeed gives a wrong picture on the lattice distortions, especially along the b direction.

To elucidate the contributions from individual species, we calculated polarizations using the structure with one sort of ion located at distorted positions obtained from the fully relaxed structure and with all the other ions located at undistorted positions.[26] Unlike the Born effective charge method in which an ion is displaced perturbatively,[29] our "site-decomposition" treatment is somewhat similar to the calculations using a hybrid lattice structure for $RMnO_3$.[30] The calculated "site-decomposed" polarizations P_{tot}, P_{ion}, and P_{ele} for each species are shown in Figs. 4(b) and 4(c). We note that because of the point charges of nuclei, the summation of P_{ion} from these "decompositions" over all ions leads to the exact $\mathbf{P}_{ion}$. However, this point-charge assumption is inappropriate for the electron cloud in the OO state. Therefore, the total $\mathbf{P}_{ele}$ cannot be retained exactly by summing over these "decomposed" P_{ele}. Nevertheless, this treatment provides a simple way to look into, at least semiquantitatively, the contributions from individual elements and would give valuable indications, as discussed below.

As shown in Fig. 4(b), Mn_{pyr} and O P_{tot} contribute the main part of the total $\mathbf{P}_{tot}$ from the GGA. The significant polarizations, particularly P_{ele}, from O actually plays the role of canceling out the Mn_{pyr} P_{ele} and leads to the small total $\mathbf{P}_{ele}$. In contrast, U of 6 eV significantly reduces polarizations from O ions [Fig. 4(c)]. This is because the two apical O4(1) and O4(2) ions of the MnO_6 octahedron [Fig. 3(c)] shift along the same direction in the GGA, whereas they move in the opposite directions in GGA+U calculations. The suppressed O P_{ele} and the fewer cancellations with Mn_{pyr} P_{ele} thus explain why the total $\mathbf{P}_{ele}$ is largely enhanced [Figs. 4(a) and 4(c)]. Furthermore, the polarizations of Mn_{oct} change sign by U due to the reduced exchange striction. Thus Mn_{pyr} P_{ion} is canceled out by Mn_{oct} and O P_{ion}, leading to the highly reduced total $\mathbf{P}_{ion}$. With $U = 6$ eV, the major components (P_{tot}) now come from Mn_{pyr} and Mn_{oct} with opposite signs. The strong cancellation hence leads to a small $\mathbf{P}_{tot}$. Besides, both P_{ion} and P_{ele} from Mn_{pyr} dominate over those from all the other ions, and give rise to the main contributions of total $\mathbf{P}_{ion}$ and $\mathbf{P}_{ele}$. This confirms the strong contribution of $Mn^{3+}O_5$ pyramids to the electronic polarization observed in optical response experiments.[24]

Finally, we would like to unravel the relation between OO and polarization. It has been demonstrated[21,22] that the electronic polarization $\mathbf{P}_{ele}$ can be calculated via the Wannier functions as

$$\mathbf{P}^{(\lambda)}_{ele} = \frac{2e}{V}\sum_{n}\int r\left|\mathcal{W}^{(\lambda)}_{n}(r)\right|^2 dr, \quad (1)$$

where e is the electron charge, V is the volume of the unit cell, λ parametrizes the displacements of atoms, and $\mathcal{W}_n^{(\lambda)}(r)$ is the nth Wannier function. Therefore, the electronic polarization can be interpreted as induced by the displacements of the center of charge of the Wannier functions. On the other hand, the transformations between the Bloch wave function and the Wannier function are

$$\mathcal{W}_n^{(\lambda)}(r) = \frac{\sqrt{V}}{(2\pi)^3} \int dk\, \psi_{nk}^{(\lambda)}(r) e^{-i\vec{k}\cdot\vec{R}} \tag{2}$$

and

$$\psi_{nk}^{(\lambda)}(r) = \sqrt{V} \sum_{\vec{R}} e^{i\vec{k}\cdot\vec{R}} \mathcal{W}_n^{(\lambda)}(r), \tag{3}$$

where $\psi_{nk}^{(\lambda)}(r)$ is the nth Bloch wave function with wave vector k. Therefore, the electronic polarization can also be presented by the Block wave functions,

$$\begin{aligned} \mathbf{P}_{ele}^{(\lambda)} &= \frac{2e}{V} \sum_n \int r \left|\mathcal{W}_n^{(\lambda)}(r)\right|^2 dr \\ &= \frac{2e}{(2\pi)^3} \sum_n \int r \int dk \left|\psi_{nk}^{(\lambda)}(r)\right|^2 dr. \end{aligned} \tag{4}$$

As a result, one can also interpret the electronic polarization as induced by the displacements of the center of charge of the Block wave functions integrated over all k. In this way, we analyze the asymmetric total valence and d_{z^2} band Bloch charge-density profiles along the b direction, and calculate the Bloch charge center shift caused by the magnetostriction-induced structure distortion. Hence the electronic polarization given from the d_{z^2} orbital can be calculated by multiplying the d_{z^2} band charge and the d_{z^2} band Bloch center shift together. Surprisingly, we found from the GGA that one d_{z^2} electron (band) yields $\sim$50% of Mn_{pyr} P_{ele}. The other three t_{2g} electrons contribute the other half of Mn_{pyr} P_{ele}. The important role of d_{z^2} OO in Mn_{pyr} P_{ele} is ascribed to the relatively high d_{z^2} band energy close to E_F and therefore the softer electron cloud that can be deformed relatively easily. In GGA+U calculations, this ratio is even higher. About 60% of P_{ele} comes from one d_{z^2} electron, which is $\sim$4.5 times larger than that from one t_{2g} electron. In particular, this Mn_{pyr} d_{z^2} electron-induced polarization is $\sim$1.5 times larger than the total $\mathbf{P}_{ele}$. The magnified contribution from the d_{z^2} electron is presumably due to the more ionic and localized picture in GGA+U since Mn_{pyr}^{3+} ions would drag the d_{z^2} electron cloud more strongly than in the GGA.

In order to test the close relation between the OO and the polarization, we have performed calculations to suppress the OO by artificially enhancing the JT distortions of the MnO_5 pyramid and by eliminating appropriate numbers of electrons in the virtual crystal approximation (VCA). In the first JT approach, we suppress the Mn-O_3 (apical) bond lengths of 1.99 Å by 0.1–0.6 Å with Mn-O_4 (O_1) (planar) bond lengths of 1.91 (1.94) Å unchanged. For the bond-length reductions of 0.1 and 0.2 Å, the d_{z^2} bands are almost fully occupied with a long tail across the Fermi level. Whereas the d_{z^2} band is significantly inhibited under a bond distance compression of 0.4 Å, resulting in a metallic state. As the Mn-O_{apical} bond length is strongly reduced by 0.6 Å, the d_{z^2} orbital is pushed above the Fermi energy and the OO is removed because of the strong Coulomb repulsion from the apical O ions. We note in this case that the Mn-O_{apical} bond length is only $\sim$1.4 Å, which is far shorter than that in real cases. Unfortunately, with d_{z^2} OO eliminated by strong JT distortion, $TbMn_2O_5$ shows conducting DOS because the $d_{x^2-y^2}$ band of the Mn_{oct} ion turns out to be partially occupied with the Fermi level crossing the band tail. Therefore, we are not able to calculate the electric polarization without OO in this manner.

In the second VCA approach, we first construct the lattice structure with Mn_{pyr} ions located at the distorted positions given from the AFM state and with all the other ions located at the undistorted positions from the FM state so that we can assure that all the effects come from the distorted Mn_{pyr} sites. This is the same as the site-decomposed polarizations method discussed in the previous paragraphs. Since the d_{z^2} band is composed of two subbands with each subband containing four electrons per unit cell, as shown in Figs. 2 and 3(a), we thus eliminate four electrons from the unit cell in the calculations to remove the higher d_{z^2} subband. This corresponds to eliminating 0.5 d_{z^2} electrons per Mn_{pyr} ion. Successfully the higher occupied d_{z^2} subband is removed with the insulating state remaining. The calculated electronic polarization (P_{ele}) given from the distorted Mn_{pyr} sites is -546 nC/cm^2. This is only $\sim$53% of the original value of -1028 nC/cm^2 from Fig. 4(b). Consequently, eliminating 50% of the d_{z^2} OO electrons would reduce $\sim$47% of P_{ele} accordingly. This clearly indicates the important role that the d_{z^2} OO plays in the electronic polarization of $TbMn_2O_5$.

To further investigate if this conclusion stands with 100% of the d_{z^2} electrons removed, we eliminate eight electrons per unit cell in the VCA calculations. This is supposed to push both the d_{z^2} subbands above the Fermi energy and totally destroy the OO state in $TbMn_2O_5$. Unfortunately, the lower d_{z^2} subband as well as the t_{2g} bands are raised up to E_F simultaneously, leading to a conducting state. We have also done GGA+U calculations with $U = 6$, 8, and 10 eV to achieve the insulating state. Nevertheless, it remains conducting even with an on-site U as large as 10 eV, so that the electric polarization is also unreachable in this case.

V. CONCLUSIONS

We have demonstrated that $TbMn_2O_5$ exhibits an insulating charge-orbital ordering ground state governed by octahedral and pyramidal crystal fields. The CO state along with the magnetostriction effect serves as the driving force of the observed ferroelectric polarization. On-site U leads to strong cancellations between $\mathbf{P}_{ion}$ and $\mathbf{P}_{ele}$, and results in a small $\mathbf{P}_{tot}$ of 83 nC/cm^2, consistent with experiment, suggesting that strong electron-electron correlation is crucial. We demonstrate that the main part of the polarizations results from the pyramidal Mn ions by analyzing the contributions from individual species. Clear evidence is presented to show that the d_{z^2} orbital ordering on the pyramidal Mn^{3+} sublattice plays important roles in the polarization.

ACKNOWLEDGMENTS

This work was supported by the National Science Council of Taiwan and Academia Sinica. We thank C.-M. Chung for fruitful discussions. We also thank NCHC, CINC-NTU, and NCTS for technical support.

*jeng@phys.sinica.edu.tw
†cyren@nknucc.nknu.edu.tw

[1] S. B. Wilkins, P. D. Spencer, P. D. Hatton, S. P. Collins, M. D. Roper, D. Prabhakaran, and A. T. Boothroyd, Phys. Rev. Lett. **91**, 167205 (2003).
[2] H.-T. Jeng, G. Y. Guo, and D. J. Huang, Phys. Rev. Lett. **93**, 156403 (2004).
[3] H.-T. Jeng, S.-H. Lin, and C.-S. Hsue, Phys. Rev. Lett. **97**, 067002 (2006).
[4] J. van den Brink and D. I. Khomskii, J. Phys. Condens. Matter **20**, 434217 (2008).
[5] K. Yamauchi and S. Picozzi, Phys. Rev. Lett. **105**, 107202 (2010).
[6] T. Kimura, T. Goto, H. Shintani, K. Ishizaka, T. Arima, and Y. Tokura, Nature (London) **426**, 55 (2003).
[7] N. Hur, S. Park, P. A. Sharma, J. S. Ahn, S. Guha, and S-W. Cheong, Nature (London) **429**, 392 (2004).
[8] L. C. Chapon, G. R. Blake, M. J. Gutmann, S. Park, N. Hur, P. G. Radaelli, and S.-W. Cheong, Phys. Rev. Lett. **93**, 177402 (2004).
[9] L. C. Chapon, P. G. Radaelli, G. R. Blake, S. Park, and S.-W. Cheong, Phys. Rev. Lett. **96**, 097601 (2006).
[10] Y. J. Choi, C. L. Zhang, N. Lee, and S.-W. Cheong, Phys. Rev. Lett. **105**, 097201 (2010).
[11] J. A. Alonso, M. T. Casais, M. J. Martínez-Lope, J. L. Martínez, and M. T. Fernández-Díaz, J. Phys. Condens. Matter **9**, 8515 (1997).
[12] J. Koo, C. Song, S. Ji, J.-S. Lee, J. Park, T.-H. Jang, C.-H. Yang, J.-H. Park, Y. H. Jeong, K.-B. Lee, T. Y. Koo, Y. J. Park, J.-Y. Kim, D. Wermeille, A. I. Goldman, G. Srajer, S. Park, and S.-W. Cheong, Phys. Rev. Lett. **99**, 197601 (2007).
[13] R. Valdes Aguilar, A. B. Sushkov, S. Park, S.-W. Cheong, and H. D. Drew, Phys. Rev. B **74**, 184404 (2006).
[14] J. Okamoto, D. J. Huang, C.-Y. Mou, K. S. Chao, H.-J. Lin, S. Park, S.-W. Cheong, and C. T. Chen, Phys. Rev. Lett. **98**, 157202 (2007).
[15] C. Wang, G.-C. Guo, and L. He, Phys. Rev. Lett. **99**, 177202 (2007).
[16] C. Wang, G.-C. Guo, and L. He, Phys. Rev. B **77**, 134113 (2008).
[17] J. P. Perdew, K. Burke, and M. Ernzerhof, Phys. Rev. Lett. **77**, 3865 (1996).
[18] A. I. Liechtenstein, V. I. Anisimov, and J. Zaanen, Phys. Rev. B **52**, R5467 (1995).
[19] P. E. Blöchl, Phys. Rev. B **50**, 17953 (1994); G. Kresse and D. Joubert, *ibid.* **59**, 1758 (1999).
[20] G. Kresse and J. Hafner, Phys. Rev. B **48**, 13115 (1993); G. Kresse and J. Furthmüller, Comput. Mater. Sci. **6**, 15 (1996); Phys. Rev. B **54**, 11169 (1996).
[21] R. D. King-Smith and D. Vanderbilt, Phys. Rev. B **47**, 1651 (1993).
[22] R. Resta, Rev. Mod. Phys. **66**, 899 (1994).
[23] We adopt the octahedral t_{2g} and e_g notations for both the Mn_{oct} and Mn_{pyr} ions.
[24] A. S. Moskvin and R. V. Pisarev, Phys. Rev. B **77**, 060102(R) (2008).
[25] S. W. Cheong and M. Mostovoy, Nat. Mater. **6**, 13 (2007).
[26] The optimized ferromagnetic structure without magnetostriction effect is taken as a reference undistorted lattice structure.
[27] G. Giovannetti and J. van den Brink, Phys. Rev. Lett. **100**, 227603 (2008).
[28] The deformations of the Mn-O-Mn atomic distances along the *a* direction are about 0.03 Å with the inversion symmetry reserved.
[29] P. Ghosez, J.-P. Michenaud, and X. Gonze, Phys. Rev. B **58**, 6224 (1998).
[30] C.-Y. Ren, Phys. Rev. B **79**, 125113 (2009).